

# First principles calculations of dopant solubility based on strain compensation and direct binding between dopants and group IV impurities

Chihak Ahn<sup>a)</sup> and Milan Diebel

Department of Physics, University of Washington, Seattle, Washington 98195

Scott T. Dunham

Department of Electrical Engineering, University of Washington, Seattle, Washington 98195

(Received 28 July 2005; accepted 30 January 2006; published 9 March 2006)

We investigated binding between dopant atoms such as boron and arsenic and various elements in group IV (e.g., C, Ge, Sn, and Pb) to explore opportunities for increasing dopant solubility, which is becoming critical for nanoscale semiconductor technology. Using first principles calculations, we find the dominant component of binding to be global strain compensation. We find negligible direct local binding between B and Ge, in contrast to some suggestions in the literature. Considering strain compensation and negative deviation from Vegard's law of lattice parameter for SiGe, we predict the enhancement of boron segregation ratio across epitaxial Si/SiGe interfaces, which agrees well with previous experimental observations. Due to nearest neighbor binding plus substantial strain compensation, Sn may have some promise for enhancing B solubility. For C/As, the first nearest neighbor interaction is repulsive. However, the large negative induced strain due to carbon overcompensates this effect in the solubility, and thus As is predicted to weakly segregate from Si into epitaxial carbon-doped Si. © 2006 American Vacuum Society. [DOI: 10.1116/1.2179458]

## I. INTRODUCTION

As the dimensions of ultra-large-scale-integrated (ULSI) devices move deeper into the nanoscale, the design window for metal oxide semiconductor transistor (MOSFET) becomes narrower. In MOSFETs with sub-100-nm channel length, short channel effects (SCEs) are a critical problem and ultra-shallow-junction (USJ) design with high dopant activation is required.<sup>1,2</sup> In modern ULSI devices, strain is incorporated both intentionally and unintentionally and can be beneficial by controlling electronic properties such as mobility and band gap, and potentially dopant redistribution as well.

There have been many experimental observations showing that B diffusion in compressively strained SiGe is retarded.<sup>3-11</sup> Local binding between B and Ge, Fermi level effects, band-gap narrowing, and strain compensations have been considered to explain B diffusion behavior in Si<sub>1-x</sub>Ge<sub>x</sub>. However, there is no consensus of explanation for dopant diffusion and activation changes with stress. Kuo *et al.* measured B diffusivity in variously strained SiGe and concluded that strain does not affect B diffusion significantly.<sup>5</sup> Lever *et al.* attributed retarded B diffusion to B/Ge pairing.<sup>4</sup> In contrast, Hattendorf *et al.* found via  $\beta$ -NMR that there is no significant binding between B and Ge.<sup>7</sup> Since diffusion is a dynamic process in which many microscopic factors are involved and the detailed mechanism (e.g., via interstitials or vacancies) of the process is also important, we focus here on segregation, which is an equilibrium process and can be explained by fundamental energy differences. In our study, we considered both stress effects and local chemical binding ef-

fects on dopant segregation. The purpose of this study was to determine whether group IV elements might be useful in enhancing dopant solubility. Combinations with compensating induced strains (B/Ge, B/Sn, B/Pb, and As/C) were selected as most likely to give significant enhancements.

## II. METHOD

The dopant concentration in strained silicon alloys can be written as

$$C_A^{\text{total}}(\epsilon) = C_A(\epsilon) + C_{AB}(\epsilon), \quad (1)$$

where  $C_A$  is the concentration of isolated dopants,  $C_{AB}$  is that of pairs of dopants and group IV impurities, and  $\epsilon$  is applied strain. Using mass action law and including first nearest neighbor (1NN) binding, the segregation ratio at the interface of strained Si<sub>1-x</sub>(Ge/Sn/Pb/C)<sub>x</sub> and unstrained Si due to group IV impurity incorporation can be approximated as

$$m = \frac{C_A^{\text{total}}(\epsilon)}{C_A(0)} \quad (2)$$

$$\approx \exp\left(-\frac{\Delta E_A^f(\epsilon)}{kT}\right) \left(1 + 4 \frac{C_B}{C_S} \left(\exp\left(-\frac{E_{AB}^b}{kT}\right) - 1\right)\right), \quad (3)$$

where  $\Delta E_A^f(\epsilon)$  is the change in formation energy of substitutional dopant due to strain and  $E_{AB}^b$  is the binding energy of dopant/group IV pair. The first exponential factor represents stress energy change due to adding dopants to strained silicon alloy, while the second term includes the effect of 1NN pairing. Using the harmonic approximation for the free energy of supercell within the elastic limit, the change in formation energy due to strain compensation is given by

<sup>a)</sup>Electronic mail: chahn@u.washington.edu

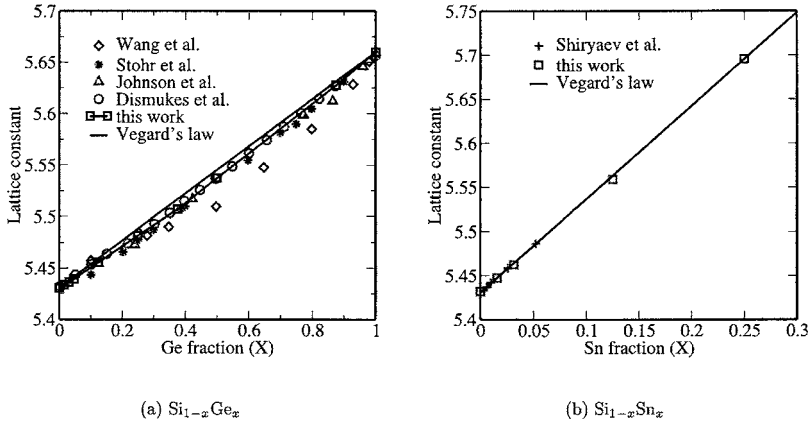


FIG. 1. Lattice constant for (a)  $\text{Si}_{1-x}\text{Ge}_x$  and (b)  $\text{Si}_{1-x}\text{Sn}_x$  vs composition. Ge shows negative deviation from Vegard's law, but Sn follows linear interpolation between Si and  $\alpha$ -Sn. DFT-GGA overestimates the lattice constant for Ge and  $\alpha$ -Sn, so end point values are normalized to experimental values for comparison to intermediate compositions.

$$\Delta E_A^f(\boldsymbol{\epsilon}) = -\Omega_0 \left( \Delta \boldsymbol{\epsilon}_A \mathbf{C}^{\text{Si}} \boldsymbol{\epsilon} + v \Delta \boldsymbol{\epsilon}_A \Delta \mathbf{C} \boldsymbol{\epsilon} - uv \frac{1}{2} \Delta \boldsymbol{\epsilon}_A \Delta \mathbf{C} \Delta \boldsymbol{\epsilon}_A \right), \quad (4)$$

where  $\Omega_0$  is the volume of a Si lattice site,  $\Delta \boldsymbol{\epsilon}_A$  is the induced strain (change in minimum energy lattice constant) due to dopant,  $\mathbf{C}^{\text{Si}}$  is elastic stiffness tensor of silicon,  $v$  and  $w$  are the concentrations of group IV impurity and dopant, respectively,  $\Delta \mathbf{C}$  is  $\mathbf{C}^{\text{Ge}} - \mathbf{C}^{\text{Si}}$ , and  $\boldsymbol{\epsilon}$  is the applied strain associated with incorporation of group IV impurities into epi-

taxial layer (detailed analysis can be found in a previous work<sup>12</sup>). The second and third terms are small and somewhat compensate each other. We include only the first term in subsequent analysis since including the last two terms in Eq. (4) has minimal effect for  $x$  less than about 0.25 as shown in Fig. 3(a). We used density functional theory generalized gradient approximation (DFT-GGA) values for  $\mathbf{C}^{\text{Si}}$  (Ref. 12) and local-density approximation (LDA) values for  $\mathbf{C}^{\text{Ge}}$ .<sup>13</sup> The applied strain  $\boldsymbol{\epsilon}$  as a function of group IV impurity composition is determined from the lattice constant of  $\text{Si}_{1-x}(\text{Ge/Sn/Pb/C})_x$ . Thus, for biaxially strained SiGe grown on top of Si ( $\boldsymbol{\epsilon} = (\epsilon_{\parallel}, \epsilon_{\parallel}, \epsilon_{\perp})$ ),

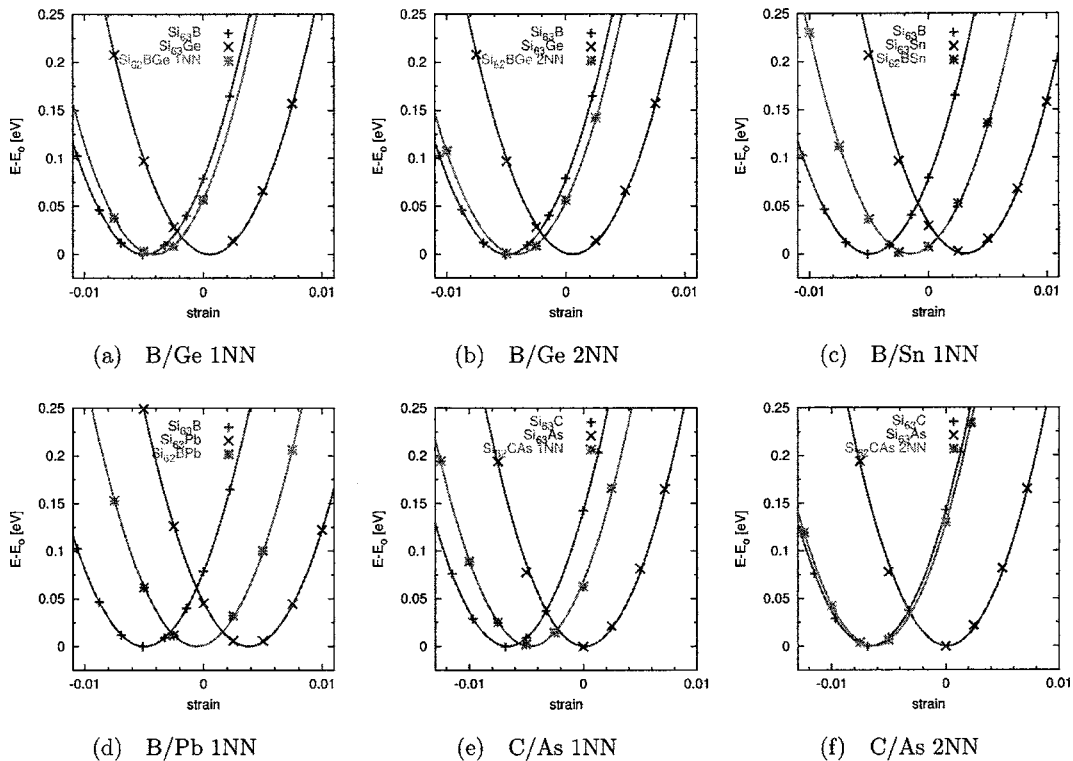


FIG. 2. Strain dependence of free energy for 64 atom supercell. Strains induced by pairs are sum of strains from isolated dopants and group IV impurities in all systems but C/As 1NN. Strains are reported in reference to the GGA Si equilibrium lattice parameter of 5.457 Å. Extracted induced strains are listed in Table I.

TABLE I. Induced strains due to dopants and group IV elements in Si. All dopant/group IV combinations considered except INN C/As show linearly additive induced strains. Strains are reported in reference to the GGA Si equilibrium lattice parameter of 5.457 Å and are normalized to Si atomic volume. Thus, the change in equilibrium lattice constant for a given composition can be obtained by summing over the induced strains times the corresponding atomic fractions.

	Si <sub>63</sub> B	Si <sub>63</sub> AS	Si <sub>63</sub> C	Si <sub>63</sub> Ge	Si <sub>63</sub> Sn	Si <sub>63</sub> Pb
$\Delta\epsilon$	-0.30	0.015	-0.42	0.051	0.21	0.26
	Si <sub>62</sub> BGe 1NN	Si <sub>62</sub> BGe 2NN	Si <sub>62</sub> BSn	Si <sub>62</sub> BPb	Si <sub>62</sub> CAs 1NN	Si <sub>62</sub> CAs 2NN
$\Delta\epsilon$	-0.24	-0.26	-0.083	-0.021	-0.29	-0.40

$$\epsilon_{\parallel} = \frac{a_{\text{Si}} - a_{\text{SiGe}}}{a_{\text{SiGe}}}, \quad \epsilon_{\perp} = -2 \frac{C_{12}}{C_{11}} \epsilon_{\parallel}. \quad (5)$$

Equation (5) has a limitation since strain-relieving defects start forming as strain becomes large. For example, Rodríguez *et al.* observed defect-free layer at  $x=0.26$  but substantial dislocation density at  $x=0.34$  (Ref. 14) in heavily B-doped Si<sub>1-x</sub>Ge<sub>x</sub>.

We calculated the total energy of 64 atom supercells with both isolated substitutional impurities as well as dopant/group IV impurity pairs under various hydrostatic strains to find induced strains, formation energies, and the lattice parameter of SiGe as a function of Ge composition using the DFT code VASP (Ref. 15) in GGA with ultrasoft Vanderbilt pseudopotentials.<sup>16</sup> Calculations were done with 340 and 345 eV energy cutoffs for boron and arsenic, respectively, and 2<sup>3</sup> Monkhorst-Pack **k**-point sampling.<sup>17</sup> The equilibrium lattice constant in Eq. (5) was taken from DFT-GGA results.

### III. RESULTS AND DISCUSSION

There have been many experiments showing that the lattice parameter of Si<sub>1-x</sub>Ge<sub>x</sub> negatively deviates from Vegard's law (linear interpolation of lattice constant between pure Si and Ge), as shown in Fig. 1.<sup>18-21</sup> Our calculations indicate that the equilibrium lattice constant of SiC shows similar behavior but with the deviation in SiC much larger than that in SiGe, in agreement with previous results.<sup>22-24</sup> As has been previously observed,<sup>25</sup> DFT-GGA overestimates the equilib-

rium lattice constant for Ge. However, the calculations accurately reproduce the experimental consensus of negative deviation from Vegard's law, as shown in Fig. 1.

Figure 2 shows the energy change versus strain for the systems considered, with the results summarized in Table I. The induced strain for all systems with exception of C/As 1NN shows linear additive behavior, which means that the total induced strain is the sum of induced strain from individual elements. For B/Ge system, we found 2NN spacing to be the minimum energy configuration, but the formation energies for B/Ge at 1NN, 2NN, and 3NN are all within 30 meV. Thus the binding energy calculated based on relaxed systems is effectively zero, with the small formation energy seen for unstrained system resulting from global strain compensation rather than any local binding. This is in contrast with some previous models proposed for B diffusion in Si<sub>1-x</sub>Ge<sub>x</sub> which assume pairing of B with Ge.<sup>4</sup> There will, however, still be segregation of B into strained SiGe on Si due to strain compensation as shown in Fig. 2(a). Our model predicts that B solubility in 1% compressively strained SiGe (corresponds to 25% Ge in Si<sub>1-x</sub>Ge<sub>x</sub>) increases to 3.5 times of that in unstrained Si, which is close to experimental<sup>6</sup> and theoretical values.<sup>26</sup>

Recently, Sadigh *et al.* and Adey *et al.* reported dopant solubility enhancement due to biaxial stress, considering strain by charged dopant and Fermi level effects.<sup>26,27</sup> They concluded that dopant solubility enhancement is caused mainly by Fermi level effects. However, Fermi level is not

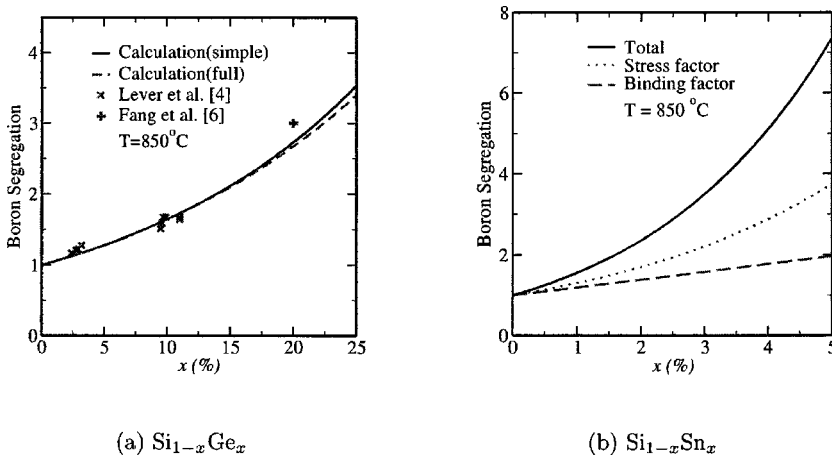


FIG. 3. Segregation of B to biaxially strained (a) SiGe and (b) SiSn on unstrained Si at 850 °C. In SiGe, segregation is just due to global strain compensation, while for SiSn, the components of segregation due to BSn 1NN pairing and strain compensation are shown separately. The predictions of calculation are in excellent agreement with experimental results of Lever *et al.* (Ref. 4) and Fang *et al.* (Ref. 6). Simple calculation includes only the first term and full calculation includes all three terms in Eq. (4). Comparing two cases at 1% strain level (25% for Ge and 5% for Sn) B/Sn pairing gives an additional boost to segregation and solubility of almost a factor 2.

TABLE II. Formation energy and binding energy between dopants and group IV elements. Formation energy ( $E^f$ ) is calculated at equilibrium lattice constant of pure Si and with isolated substitutional impurities as reference. Binding energy ( $E^b$ ) is calculated with relaxed (lowest energy) lattice constants and thus excludes global stress compensation. For B/Ge and C/As the 2NN configuration has larger binding energy than other configurations.

	Si <sub>62</sub> BGe 1NN	Si <sub>62</sub> BGe 2NN	Si <sub>62</sub> BSn	Si <sub>62</sub> BPb	Si <sub>62</sub> CAs 1NN	Si <sub>62</sub> CAs 2NN
$E^f$ (eV)	-0.009	-0.038	-0.27	-0.36	0.10	-0.078
$E^b$ (eV)	0.016	-0.016	-0.17	-0.23	0.17	-0.064

independent of strain since charged carriers induce strain, which is explained by deformation potential.<sup>28,29</sup> We found that strain due to neutral dopant is the sum of strain due to charged dopant and electron or hole. For instance, the lattice contractions caused by a B<sup>-</sup> and a hole are -0.032 and -0.27, respectively. Therefore, our description using neutral B already includes Fermi level effects.

As seen in Fig. 2 and Table I, Sn and Pb both produce much larger induced strains than Ge. The same analysis done for B/Ge is applied to these systems, and the results are summarized in Figs. 2 and 3(b) and Tables I and II. Again, DFT-GGA overestimates the lattice constants. The lattice constant of Si<sub>1-x</sub>Sn<sub>x</sub> follows Vegard's law, consistent with experiment [Fig. 1(b)]. In these systems, 1NN is the most favorable configuration, suggesting the possibility of local binding. This is confirmed by the calculation results which show binding energies of -0.17 and -0.23 eV for B with Sn and Pb, respectively, based on relaxed cells.

To investigate the electronic properties of B/Sn pairs, we looked at the calculated density of states (DOS) of Si<sub>62</sub>BSn and compared it to DOS of Si<sub>63</sub>B (Fig. 4). The DOS is nearly unchanged, with the empty state present at the top of the valence band indicating that B/Sn pairs act as shallow acceptors. Considering the large induced positive strain and additional direct binding, Sn is a potentially promising element for enhancing boron solubility. Although equilibrium

solubility of Sn in Si is only about 0.1%, Sn can be introduced in Si up to 5%.<sup>30</sup> Such condition has similar strain to Si<sub>0.75</sub>Ge<sub>0.25</sub>, but the local binding increases solubility by an additional factor of 2. Pb has slightly larger local binding and induced strain than Sn, but it is less likely to be useful for enhancing B activation since the solid solubility of Pb is extremely low.<sup>31</sup>

To connect the segregation enhancement to the change in activation, we must consider strain effects on boron interstitial clusters (BICs), since the coexistence of BICs with isolated boron determines the equilibrium solubility limit (ESL), which is about 10<sup>20</sup> cm<sup>-3</sup> at 1000 °C.<sup>32</sup> Induced strain per boron atom due to BICs (e.g., B<sub>3</sub>I and B<sub>12</sub>I<sub>7</sub>) is much smaller than for isolated boron.<sup>12</sup> Thus, the change in strain energy due to forming a BIC is nearly equal to that due to elimination of the substitutional B.<sup>33</sup> Neglecting incorporation of Ge into BICs (which we find energetically unfavorable), the change in activation between Si and strained SiGe then nearly equals the segregation ratio [Fig. 3(a)].

We also investigated strain compensation binding for *n*-type doping via pairing of C with As. In contrast to reported lattice contraction due to incorporation of As by Cargill III *et al.*,<sup>28</sup> *ab initio* calculation predicts a slight lattice expansion, but the mismatch is very small, and experimental results may be explained by the negative induced strain due to As<sub>m</sub>V<sub>n</sub> cluster formation. We found that C-As

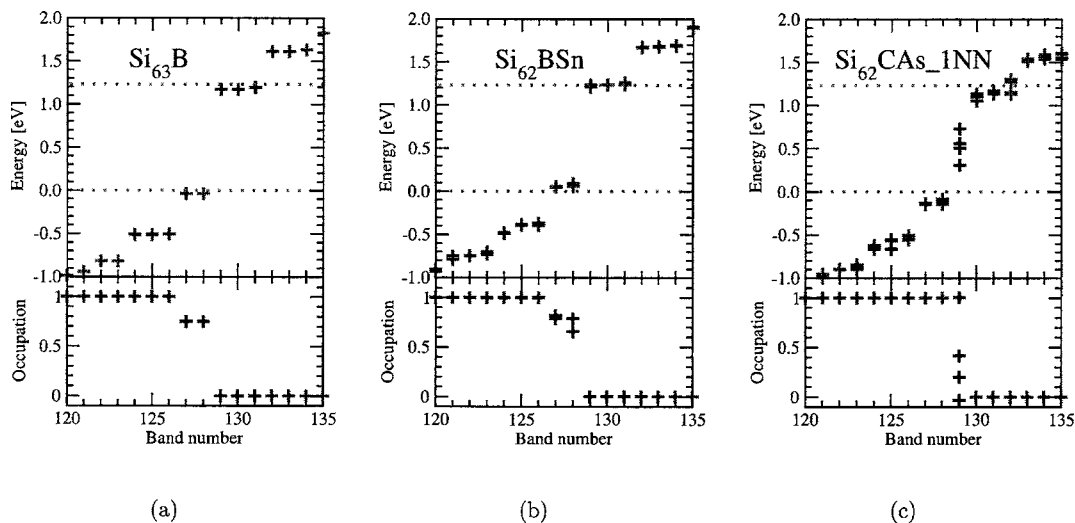


FIG. 4. Comparison of the density of states of (a) Si<sub>63</sub>B<sup>0</sup> and (b) Si<sub>62</sub>BSn<sup>0</sup> with 2<sup>3</sup> k-point sampling, showing that they are both shallow acceptors [note empty state at the valence band maximum (lower broken line)]. In contrast (c) DOS indicates that As in Si<sub>62</sub>CAs<sup>0</sup> is not a shallow donor, as seen by partially filled states between conduction band minimum (upper broken line) and valence band maximum.

pairs repel each other at 1NN and the complex SiCAs is not a shallow donor [Fig. 4(c)], while 2NN and 3NN interactions are attractive. Overall, we believe that As still segregates into tensilely strained  $\text{Si}_{1-x}\text{C}_x$  for small  $x$  due to strain compensation and weak 2NN and 3NN attractive binding, consistent with Sadigh *et al.*<sup>26</sup> and Adey *et al.*<sup>27</sup>

#### IV. CONCLUSION

Dopant segregation ratios at the interface of  $\text{Si}/\text{Si}_{1-x}(\text{Ge}/\text{Sn}/\text{Pb}/\text{C})_x$  were predicted using *ab initio* DFT calculations and compared to experimental observations. In contrast to previous suggestions,<sup>4</sup> we found that the segregation of B into compressively strained SiGe can be fully explained by global strain compensation without local binding. Because of minimal induced strain per B atom for boron interstitial clusters, we expect the segregation ratio to translate to nearly equivalent solubility enhancement. We predict that the additional local binding energy between B and Sn can enhance boron solubility significantly in  $\text{Si}_{1-x}\text{Sn}_x$ , with some promise for enhancing activation. C/As shows complicated behavior with 1NN repulsion, but we believe that strain compensation and longer range attraction indicate that C enhances As solubility. The calculation results can be extended to arbitrary stress/alloy conditions via application of Eq. (3) and the values in Tables I and II.

#### ACKNOWLEDGMENTS

This research was funded by the Semiconductor Research Corporation. Most of the calculations were conducted on computers hardware donated by Intel and AMD. The authors thank J. Song for valuable discussions.

This paper was presented at the Eight International Workshop on Fabrication, Characterization, and Modeling of Ultra-Shallow Doping Profiles in Semiconductors (USJ-2005) June 5–8, 2005 in Dayton Beach, FL.

<sup>1</sup>E. C. Jones and E. Ishida, *Mater. Sci. Eng., R.* **24**, 1 (1998).

<sup>2</sup>M. Jeong, B. Doris, J. Kedzierski, K. Rim, and M. Yang, *Science* **306**, 2057 (2004).

<sup>3</sup>S. M. Hu, D. C. Ahlgren, P. A. Ronsheim, and J. O. Chu, *Phys. Rev. Lett.* **67**, 1450 (1991).

<sup>4</sup>R. F. Lever, J. M. Bonar, and A. F. W. Willoughby, *J. Appl. Phys.* **83**, 1988 (1998).

<sup>5</sup>P. Kuo, J. L. Hoyt, J. F. Gibbons, J. E. Turner, and D. Lefforge, *Appl. Phys. Lett.* **66**, 580 (1995).

<sup>6</sup>T. T. Fang, W. T. C. Fang, P. B. Griffin, and J. D. Plummer, *Appl. Phys. Lett.* **68**, 791 (1996).

<sup>7</sup>J. Hattendorf, W.-D. Zeitz, W. Schröder, and N. V. Abrosimov, *Physica B* **340–342**, 858 (2003).

<sup>8</sup>K. Rajendran and W. Schoenmaker, *J. Appl. Phys.* **89**, 980 (2001).

<sup>9</sup>C.-H. Chen, U. M. Gösele, and T. Y. Tan, *Appl. Phys. A: Mater. Sci. Process.* **68**, 19 (1999).

<sup>10</sup>N. Moriya, L. C. Feldman, H. S. Luftman, C. A. King, J. Bevk, and B. Freer, *Phys. Rev. Lett.* **71**, 883 (1993).

<sup>11</sup>N. E. B. Cowern, P. C. Zalm, P. van der Sluis, D. J. Gravesteijn, and W. B. de Boer, *Phys. Rev. Lett.* **72**, 2585 (1994).

<sup>12</sup>M. Diebel, Ph.D. thesis, University of Washington, 2004.

<sup>13</sup>N. Bernstein, M. J. Mehl, and D. A. Papaconstantopoulos, *Phys. Rev. B* **66**, 075212 (2002).

<sup>14</sup>A. Rodríguez, T. Rodríguez, A. Kling, J. C. Soares, M. F. da Silva, and C. Ballesteros, *J. Appl. Phys.* **82**, 2887 (1997).

<sup>15</sup>G. Kresse and J. Hafner, *Phys. Rev. B* **47**, RC558 (1993); G. Kresse and J. Furthmüller, *ibid.* **54**, 11169 (1996).

<sup>16</sup>D. Vanderbilt, *Phys. Rev. B* **41**, 7892 (1990); G. Kresse and J. Hafner, *J. Phys.: Condens. Matter* **6**, 8245 (1994).

<sup>17</sup>A. Baldereschi, *Phys. Rev. B* **7**, 5212 (1973); D. J. Chadi and M. L. Cohen, *ibid.* **8**, 5747 (1973); H. J. Monkhorst and J. D. Pack, *ibid.* **13**, 5188 (1976).

<sup>18</sup>J. P. Dismukes, L. Ekstrom, and R. J. Paff, *J. Phys. Chem.* **68**, 3021 (1964).

<sup>19</sup>H. Stohr and W. Klemm, *Z. Anorg. Allg. Chem.* **241**, 313 (1939).

<sup>20</sup>E. R. Johnson and S. M. Christian, *Phys. Rev.* **95**, 560 (1954).

<sup>21</sup>C. C. Wang and B. H. Alexander, Bureau of Ships Final Technical Report No. **NObsr-63180**, 1955 (unpublished).

<sup>22</sup>M. Berti, D. De Salvador, A. V. Drigo, F. Romanato, J. Stangi, S. Zerlauth, F. Schäffler, and G. Bauer, *Appl. Phys. Lett.* **72**, 1602 (1998).

<sup>23</sup>P. C. Kelires, *Phys. Rev. B* **55**, 8785 (1997).

<sup>24</sup>J. Martins and A. Zunger, *Phys. Rev. Lett.* **56**, 1400 (1986).

<sup>25</sup>S. Lee, J. Kang, and M. Kang, *J. Korean Phys. Soc.* **31**, 811 (1997).

<sup>26</sup>B. Sadigh *et al.*, *Appl. Phys. Lett.* **80**, 4738 (2002).

<sup>27</sup>J. Adey, R. Jones, and P. R. Briddon, *Phys. Status Solidi C* **2**, 1953 (2005).

<sup>28</sup>G. S. Cargill III, J. Angillelo, and K. J. Kavanagh, *Phys. Rev. Lett.* **61**, 1748 (1988).

<sup>29</sup>M. Leszczynski, J. Bak-Misiuk, J. Domagala, J. Muszalski, M. Kaniewska, and J. Marczewski, *Appl. Phys. Lett.* **67**, 539 (1995).

<sup>30</sup>S. Yu. Shiryayev, J. Lundsgaard Hansen, P. Kringhoj, and A. Nylandsted Larsen, *Appl. Phys. Lett.* **67**, 2287 (1995).

<sup>31</sup>J. S. Williams, *Nucl. Instrum. Methods Phys. Res.* **209**, 219 (1983).

<sup>32</sup>S. Solmi, F. Baruffaldi, and R. Canteri, *J. Appl. Phys.* **69**, 2135 (1991).

<sup>33</sup>M. Diebel, S. Chakravarthi, S. T. Dunham, and C. F. Machala, *Proceedings of the International Conference on Simulation of Semiconductor Processes and Devices, SISPAD 2004*, Munich, Germany, 2–4 September 2004 (IEEE, New York, 2004), pp. 37–40.